Noise Estimation for Color Edge Extraction

Regine Brügelmann, Wolfgang Förstner

Institut für Photogrammetrie
Universität Bonn
Nußallee 15, D – 5300 Bonn 1
Tel. 0228-732713; FAX 0228-733281

Abstract

The paper discusses an automatic procedure for color edge extraction. It contains a procedure for robustly estimating the signal dependent components of the noise which is assumed to be influenced mainly by the Poisson statistics of the photon radiance. This allows to mutually weight different channels of a multispectral image. Except for a significance level no other tresholds are required.

1 Introduction

The essential first step in data reduction for automatic image interpretation is the description of images by elementary image structures such as characteristic points, edges or homogeneous areas. Among these, edges will be the subject of the following discussion. We will comprehend edge extraction as the transition from a digital gray–level image to a digital binary representation, only containing potential edge pixels, and finally proceed to a symbolic image description with lists, graphs and relations.

The majority of known edge detection algorithms treats edge extraction in gray–level images (cf. e.g. YAKIMOVSKY 1976, CHEN 1981, DE SOUZA 1983, HSU/NAGEL/REKERS 1984, SUK 1984, SHIOZAKI 1986, TORRE 1986). Transfering ideas of such algorithms to multichannel images might be useful because adding color information may facilitate scene reconstruction. E.g. imagine you want to extract house contours out of a gray–level image. Then the edge detection algorithm not only determines the house contours but also its shadow outlines. Color information would obviously help to seperate house and shadow outlines (cf. NEVATIA 1977, SOLINSKY 1985, DREWNIOK 1988).

In image analysis and especially edge detection one always must take into account the effect of noise. It is caused by various disturbing effects of the imaging process and creates random fluctuations in image intensities. The question now is whether detected gray–level differences appear due to noise on the one hand or due to real edges on the other hand. To solve this problem usually a treshold is introduced to seperate noise and edges. This approach actually is a hypothesis test to check the significance of local changes in image structure.

For this purpose the signal and noise characteristics have to be known as reliable as possible. It is common practice to parametrize signal and noise characteristics and to derive the unknown parameters from the image content, thus adapting the image model to the actual data. Whereas models and estimation procedures for image signals are quite advanced, models for image noise as well the corresponding estimates are still very simple, usually restricted to white noise with signal independent variance. This paper, therefore, mainly deals with extending the noise model, deriving automatic procedures for estimating the main parameters and uses it for the problem of color edge extraction as one example for application.
Section 2 discusses the assumed image model, especially the statistical properties of the noise component containing the photon noise which is Poisson distributed and therefore leads to a signal dependent noise variance. In section 3 a robust procedure for estimating the variance–components of the noise in presence of disturbing edges or limited texture. Section 4 describes how this technique may be used to weight the channels of a multispectral image with respect to each other during color edge extraction, generalizing the approach of CUMANI (1989).

2 Models

In order to arrive at a procedure for color edge extraction which can be evaluated we need to specify the assumed model. It is based on an image model which under certain conditions may be derived from an object model using geometric and physical properties of the imaging process. The statistical properties of the observable image intensities are essential for fixing illumination and reflectance independent tresholds in the edge extraction process and properly weighting the information of the different channels.

2.1 Object model

We assume the world to consist of objects which have the following properties:

1. The objects are bounded by piecewise smooth surfaces which themselves are bounded by piecewise smooth lines.

2. The reflectance properties vary piecewise smoothly.

This model excludes objects with — compared with the image resolution — rough surfaces or very irregular texture. A formal description of the smoothness requirements is given in the image model.

2.2 Image model

The image then can be described in the following way (cf. e.g. CHEN/PAVLIDIS 1987). Let the image I be composed of mutually exclusive segments of homogeneous regions $R = \{R_i\}$, $i = 1, \ldots, n$ and of boundary regions $B = \{B_j\}$, $j = 1, \ldots, m$ with

$$I = B \cup R = \{B_i\} \cup \{R_j\}. \tag{1}$$

The segmentation thus requires a homogeneity measure h. In case of edge free areas this measure should be governed by the noise component alone allowing to robustly estimating the noise variance.

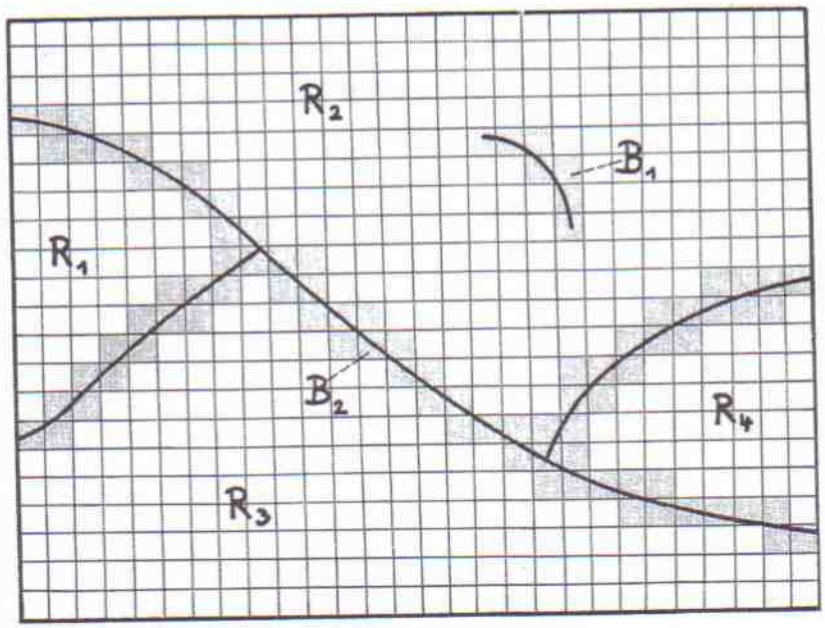

Figure 1: Image Model

Thus the segmentation may be interpreted as a hypothesis test with the hypothesis:

H_0: point $\mathbf{x}$ belongs to a homogeneous region[1]

H_a: point $\mathbf{x}$ does not belong to a homogeneous region (boundary region)

Thus boundary regions are defined in a negative manner. A, possibly vector valued, homogeneity measure $\underline{h}$ may be used to test H_0 against H_a. According to NEYMAN and PEARSON (1933) a most powerful test would discern H_0 and H_a by fixing the probability α for a type I error (erroneously rejecting H_0) and choosing a critical region for $\underline{h}$ which minimizes the probability $1-\beta$ for a type II error (erroneously accepting H_0). In order to develop such a test one needs the statistical properties of the data from which the distribution of $\underline{h}$ may then be derived.

2.3 Signal and noise model

We assume the observed image intensities $\mathbf{g}$ to be a contaminated version of the true signal $\mathbf{f}$

$$\underline{\mathbf{g}}(\mathbf{x}) = \underline{\mathbf{f}}(\mathbf{x}) + \underline{\mathbf{n}}(\mathbf{x}) \tag{2}$$

The N_k spectral components $k = 1, \ldots, N_k$ of $\underline{\mathbf{g}}(\mathbf{x}), \underline{\mathbf{f}}(\mathbf{x})$ and the noise $\underline{\mathbf{n}}(\mathbf{x})$ are denoted by $\underline{\mathbf{g}}_k(\mathbf{x}), \underline{\mathbf{f}}_k(\mathbf{x})$ and $\underline{\mathbf{n}}_k(\mathbf{x})$[2]. We assume the true function $\underline{\mathbf{f}}$ to vary smoothly almost

[1] $\mathbf{x} \equiv (x_1, x_2) = (r, c)$

[2] stochastical variables are underscored

everywhere, namely at edges or possibly in a few textured areas. The smoothness may be measured either by the first or the second derivatives. In both cases we assume on an average the expectation of the derivatives to be zero and the variance of the derivatives to be small compared with the variance of the corresponding derivatives of the noise.

$$\text{Model A:} \qquad \left.\begin{aligned} E\left(\frac{\partial \underline{f}}{\partial x_i}\right) &= 0 \\ D\left(\frac{\partial \underline{f}}{\partial x_i}\right) &\ll D\left(\frac{\partial \underline{n}}{\partial x_i}\right) \end{aligned}\right\} \quad x \in R \tag{3}$$

$$\text{Model B:} \qquad \left.\begin{aligned} E\left(\frac{\partial^2 \underline{f}}{\partial x_i \partial x_j}\right) &= 0 \\ D\left(\frac{\partial^2 \underline{f}}{\partial x_i \partial x_j}\right) &\ll D\left(\frac{\partial^2 \underline{n}}{\partial x_i \partial x_j}\right) \end{aligned}\right\} \quad x \in R \tag{4}$$

where the derivatives have to be interpreted as the discrete approximations using an appropriate convolution kernel.
No assumption on the correlation between neighbouring $\underline{\mathbf{f}}(\mathbf{x})$ is made. No specification in the boundary areas is made for the noise estimation process. The color edge extraction process however needs a model for the boundary regions. As our main concern in this paper is the identification of the noise characteristics and the automatic edge detection, not the edge location as such, we apply a simple edge model: neighbouring homogeneous regions are assumed to be linked by a blurred step edge, where the kernel of the blurring filter is a symmetric bellshaped function (cf. section 4).
We assume the noise component $\underline{\mathbf{n}}$ to be statistically independent on $\underline{\mathbf{f}}$ and white, thus being spatially uncorrelated with $E(\underline{\mathbf{n}}) = \mathbf{0}$. It can be assumed to be additively composed of two independent components

$$\underline{\mathbf{n}} = \underline{\mathbf{n}}^{(1)} + \underline{\mathbf{n}}^{(2)}, \tag{5}$$

$\underline{\mathbf{n}}^{(1)}$ having a signal independent variance

$$\mathbf{\Sigma}_{11} = \mathbf{A} \tag{6}$$

covering electronic noise or rounding errors. $\underline{\mathbf{n}}^{(2)}$ may be written as

$$\underline{\mathbf{n}}^{(2)} = \mathbf{M} \cdot \underline{\mathbf{s}} \tag{7}$$

where $\underline{\mathbf{s}}$ are n_s independent noise sources and $\mathbf{M}$ some influence factors. Then

$$\mathbf{\Sigma}_{22} = \mathbf{M} \cdot \mathbf{\Sigma}_{ss} \cdot \mathbf{M}^{\mathsf{T}}. \tag{8}$$

The determination of the number n_s of noise sources of the influence matrix $\mathbf{M}$ and of $\mathbf{A}$ has to be determined by a proper calibration of the camera. In case the noise sources $\underline{\mathbf{s}}$ are the photon fluxes in the N_k channels, $\mathbf{M}$ can be assumed to be diagonal $\mathbf{M} = Diag(m_k)$ which results in

$$\mathbf{\Sigma}_{22} = Diag(m_k \cdot \sigma_{s_k}^2) \tag{9}$$

with $\sigma^2_{s_k}$ proportional to $s_k = f_k$ due to the Poisson distribution of the number of photons received. This leeds to

$$\Sigma_{nn}(\mathbf{x}) = \mathbf{A} + Diag(b_k \cdot \underline{f}_k(\mathbf{x})) = \mathbf{A} + \mathbf{B}(\underline{\mathbf{f}}(\mathbf{x})) \tag{10}$$

or, if the channels are independent,

$$\sigma^2_{n_k}(\mathbf{x}) = a_k + b_k \cdot \underline{f}_k(\mathbf{x}), \qquad k = 1, \ldots, N_k \tag{11}$$

For large enough numbers of photons the Poisson distribution may reliably be approximated by a Gaussian distribution. Thus we finally have the noise distribution

$$\underline{\mathbf{n}}(\mathbf{x}) \sim N\big(0, \mathbf{A} + \mathbf{B}(\underline{\mathbf{f}}(\mathbf{x}))\big) \tag{12}$$

or with independent noise components

$$n_k(\mathbf{x}) \sim N\big(0, a_k + b_k \cdot \underline{f}_k(\mathbf{x})\big). \tag{13}$$

For practical purposes always $f_k \approx g_k$ can be assumed. Observe that this model contains the assumed dependency of the noise variance on both the channel and the location within the image.

2.4 Homogeneity measures and their statistics

The homogeneity measure used for the segmentation has to fulfill three criteria:

a) It should not be influenced by the local variations in the smooth areas.

   Using the signal models A and B, this requires to base the homogeneity measure on deviations from a horizontal or tilted plane through the intensities of a small neighbourhood. This is closely related to the facet model (cf. HARALICK 1981, DE SOUZA 1983, HSU/NAGEL/REKERS 1984).

b) It should not be influenced by edges or other strong deviations from the assumed model.

   This requires a robust estimation procedure for the variance components **A** and **B**, which will be discussed in the next section.

c) Its statistical properties should be derivable at least approximately.

   In case the homogeneity measure would be based only on homogeneous regions its distribution should be determinable rigorously.

We therefore use the following kernels for deriving the homogeneity:

$$\text{model A:} \qquad u^{(A)} = \begin{pmatrix} 0 & 0 & 0 \\ -1 & 0 & 1 \\ 0 & 0 & 0 \end{pmatrix} \qquad v^{(A)} = \begin{pmatrix} 0 & 1 & 0 \\ 0 & 0 & 0 \\ 0 & -1 & 0 \end{pmatrix} \tag{14}$$

$$\text{model B:} \quad u^{(B)} = \begin{pmatrix} 1 & 0 & -1 \\ 0 & 0 & 0 \\ -1 & 0 & 1 \end{pmatrix} \qquad v^{(B)} = \begin{pmatrix} 0 & 1 & 0 \\ -1 & 0 & -1 \\ 0 & 1 & 0 \end{pmatrix} \tag{15}$$

In both cases ($*$ = symbol for convolution)

$$E(u * \underline{\mathbf{g}}(\mathbf{x})) = E(v * \underline{\mathbf{g}}(\mathbf{x})) = \mathbf{0}, \qquad \mathbf{x} \in R. \tag{16}$$

holds. The variances are

$$\text{model A:} \quad V(u * \underline{\mathbf{g}}(\mathbf{x})) = V(v * \underline{\mathbf{g}}(\mathbf{x})) = 2\boldsymbol{\Sigma}_{nn}(\mathbf{x}) = 2(\mathbf{A} + \mathbf{B}(\mathbf{f}(\mathbf{x}))) \tag{17}$$

$$\text{model B:} \quad V(u * \underline{\mathbf{g}}(\mathbf{x})) = V(v * \underline{\mathbf{g}}(\mathbf{x})) = 4\boldsymbol{\Sigma}_{nn}(\mathbf{x}) = 4(\mathbf{A} + \mathbf{B}(\mathbf{f}(\mathbf{x}))) \tag{18}$$

and

$$\mathbf{Cov}(u * \underline{\mathbf{g}}(\mathbf{x}), v * \underline{\mathbf{g}}(\mathbf{x})) = \mathbf{0} \tag{19}$$

for both models. Therefore the homogeneity measure

$$\underline{h}^2(\mathbf{x}) = \|u * \underline{\mathbf{g}}(\mathbf{x})\|_w^2 + \|v * \underline{\mathbf{g}}(\mathbf{x})\|_w^2 \tag{20}$$

with $\|\mathbf{a}\|_w^2 = \mathbf{a}^\top \mathbf{W} \mathbf{a}$ and

$$\mathbf{W} = \left[t/2\ \boldsymbol{\Sigma}_{nn}(\mathbf{x})\right]^{-1} \tag{21}$$

is $\chi^2_{2N_k}$ distributed with

$$t = 4 \qquad \text{model A} \tag{22}$$

$$t = 8 \qquad \text{model B} \tag{23}$$

in case $\mathbf{x} \in R$ and in case of N_k spectral channels involved. Thus

$$\begin{array}{rcl} E(\underline{h}^2(\mathbf{x})) & = & 2N_k \\ V(\underline{h}^2(\mathbf{x})) & = & 4N_k \end{array}, \qquad \mathbf{x} \in R \tag{24}$$

for both models. In case of a single channel we could simplify to ($N_k = 1$):

$$\begin{array}{rcl} E\left(\|u * \underline{g}(\mathbf{x})\|^2 + \|v * \underline{g}(\mathbf{x})\|^2\right) & = & t\left(a + b\underline{f}(\mathbf{x})\right) \\ V\left(\|u * \underline{g}(\mathbf{x})\|^2 + \|v * \underline{g}(\mathbf{x})\|^2\right) & = & t^2\left(a + b\underline{f}(\mathbf{x})\right)^2 \end{array}, \qquad \mathbf{x} \in R. \tag{25}$$

Eq.(25) is the basis for the estimation of a and b discussed in the next section.

3 Noise estimation

The estimation of the noise variance parameters $\mathbf{A}$ and $\mathbf{B}$ can be based on eq. (16–19). In case of correlated channels this would require the estimation of variance components in a multivariate model. We want to restrict the discussion to the case where the channels are uncorrelated. Then eq. (25) can be interpreted as a nonlinear Gauß–Markov–Model (GMM):

$$E(\underline{y}_i) = \left(1\ \underline{f}(\mathbf{x}_i)\right) \cdot \left(\beta_1\ \beta_2\right)^\top \tag{26}$$

$$V(\underline{y}_i) = \sigma_i^2 \qquad , \quad i \in R \tag{27}$$

$$\text{with} \quad \boldsymbol{\beta}^\top = \left(\beta_1\ \beta_2\right)^\top = t\left(a\ b\right)^\top \tag{28}$$

$$\underline{y}_i = \left(\|u * \underline{g}(\mathbf{x}_i)\|^2 + \|v * \underline{g}(\mathbf{x}_i)\|^2\right) \tag{29}$$

$$\sigma_i^2 = t^2(\beta_1 + \beta_2 \cdot \underline{f}(\mathbf{x}_i))^2. \tag{30}$$

Comparing eq. (20) and (29) shows $\underline{y}_i = h(\mathbf{x}_i)/\sqrt{w(\mathbf{x}_i)}$. Eq. (30) reveils the model being nonlinear as the variance depends on the unknown parameters. A second nonlinearity results from the fact that $\underline{\mathbf{f}}(\mathbf{x})$ is not known but has to be predicted from $\underline{\mathbf{g}}(\mathbf{x})$. We use the approximation $\underline{\mathbf{f}}(\mathbf{x}) \approx \underline{\mathbf{g}}(\mathbf{x})$ in the following.
As the model eq. (26, 27) only refers to pixels in the homogeneous regions $\{R_i\}$ a robust estimation for β_1 and β_2 has to be developed. We apply the following steps:

1. Determination of robust initial values $\boldsymbol{\beta}^{(0)}$ and extracting the 50% most homogeneous pixels.

2. Estimating the parameters $\boldsymbol{\beta}^{(1)}$ using these best pixels based on the GMM and correcting for bias due to truncation of the distribution.

This procedure is a generalization of the one given by FÖRSTNER (1991) for the constant noise case. It is applied to the channels individually.

3.1 Approximate values for β

The approximate values should be

a) accurate and

b) robust with respect to edges in the image.

This can be achieved by using the δ, say 10%, smallest and largest intensities and determining the median both for g_j and y_j within both groups, leading to

$$g_s = med_S(g_j) \qquad S = \{i \mid g_i < g_\delta\} \tag{31}$$

$$y_s = med_S(y_j) \tag{32}$$

$$\text{and} \quad g_l = med_L(g_j) \qquad L = \{i \mid g_i > g_{1-\delta}\} \tag{33}$$

$$y_l = med_L(y_j) \tag{34}$$

with g_δ being the δ–point of the distribution of g. This leads to the approximate values

$$\beta_2^{(0)} = \frac{y_l - y_s}{g_l - g_s} \tag{35}$$

$$\beta_1^{(0)} = y_s - b^{(0)} \cdot g_s \,. \tag{36}$$

Using the extrema of the histogram results in a stable solution, especially for $\beta_2^{(0)}$. Using the median, both for g and y, results in robustness against both, single extreme values g_i in the histogram and inhomogeneous pixels.
Remark: Using $\delta = 0.5$ lead to difficulties in images with a small homogeneous object on a homogeneous background, as the medians g_l and g_s were very close, resulting in instabilities of $\beta_2^{(0)}$.
In order to reliably eliminate edge pixels from the estimation process the homogeneities y_i are compared with their corresponding standard deviation, derivable from (27). We

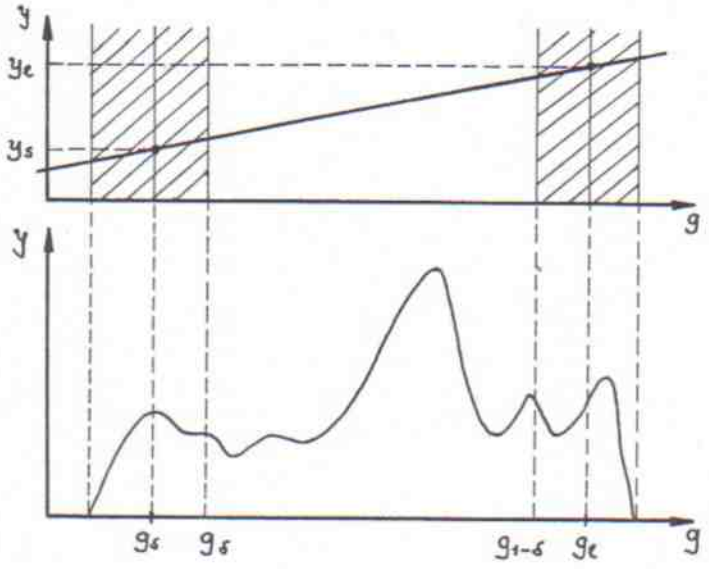

Figure 2: Scatter diagram of (g_i, y_i)

therefore obtain the set H of homogeneous pixels from

$$H = \{i \mid y_i/\sigma_{y_i} < med_j(y_j/\sigma_{y_j})\} \quad (37)$$

$$= \{i \mid h_i^2 < med_j(h_j^2)\} \quad (38)$$

$$\text{with} \quad \sigma_{y_i}^2 = \beta_1^{(0)} + \beta_2^{(0)} \cdot g(\mathbf{x}_i) \quad (39)$$

and h_i^2 from eq. (20). Thus the set H contains the 50% most homogeneous pixels. It is assumed that all major edge pixels are eliminated this way, and the edge pixels with very low contrast will not deteriorate the following fine–estimation process.

3.2 Estimating the noise variance parameters

The final estimation of the noise parameters is based on the 50% most homogeneous pixels using the GMM eq. (26, 27). It leads to the normal equations

$$\mathbf{N}^{(\nu)} \cdot \boldsymbol{\beta}^{(\nu+1)} = \mathbf{h}^{(\nu)}, \qquad \nu = 0, 1, \ldots \quad (40)$$

$$\text{with} \quad \mathbf{N}^{(\nu)} = \begin{pmatrix} \sum_i \frac{1}{t^2\left(\beta_1^{(\nu)} + \beta_2^{(\nu)} g(\mathbf{x}_i)\right)^2} & \sum_i \frac{g(\mathbf{x}_i)}{t^2\left(\beta_1^{(\nu)} + \beta_2^{(\nu)} g(\mathbf{x}_i)\right)^2} \\ \sum_i \frac{g(\mathbf{x}_i)}{t^2\left(\beta_1^{(\nu)} + \beta_2^{(\nu)} g(\mathbf{x}_i)\right)^2} & \sum_i \frac{g^2(\mathbf{x}_i)}{t^2\left(\beta_1^{(\nu)} + \beta_2^{(\nu)} g(\mathbf{x}_i)\right)^2} \end{pmatrix} \quad (41)$$

$$\mathbf{h}^{(\nu)} = \begin{pmatrix} \sum_i \frac{y_i}{t^2\left(\beta_1^{(\nu)} + \beta_2^{(\nu)} g(\mathbf{x}_i)\right)^2} \\ \sum_i \frac{y_i g(\mathbf{x}_i)}{t^2\left(\beta_1^{(\nu)} + \beta_2^{(\nu)} g(\mathbf{x}_i)\right)^2} \end{pmatrix}, \qquad i \in H \quad (42)$$

The variances of $\hat{\beta}$ may be determined from

$$\hat{\Sigma}_{\hat{\beta}\hat{\beta}} = \hat{\sigma}_0^2 \cdot \mathbf{N}^{-1} \tag{43}$$

$$\text{with} \quad \hat{\sigma}_0^2 = \sum_i \left[y_i - (\hat{\beta}_1 + \hat{\beta}_2 \cdot g(x_i))\right]^2 / (|H| - 2)\,. \tag{44}$$

The iterations process usually converges quickly, two iterations in almost all cases have shown to be sufficient. The results of this iteration process are the estimates $\beta^{(g)}$.
The parameters $\beta^{(g)}$ are biased for two reasons:

a) only the best 50% of the data is used

b) the true percentage of non homogeneous pixels is not known.

We therefore first compensate for using only half the data:

$$\beta^{(h)} = c_1 \cdot \beta^{(g)} \tag{45}$$

$$\text{with} \quad c_1 = 1/(1 - ln2). \tag{46}$$

The estimates $\beta^{(h)}$ are not influenced by non–homogeneous regions, but the correction factor c_1 is too large, as the non–homogeneous pixels are assumed to solely consist of (large) noise. Therefore, we estimate the percentage $1 - \alpha$ of homogeneous pixels using the estimates $\beta^{(h)}$:

$$H(\alpha') = \{i \mid y_i/\sigma_{y_i} < \chi^2_{2,1-\alpha'}\} \tag{47}$$

with $\chi^2_{2,1-\alpha'}$ being the $(1-\alpha')$–point of the χ^2_2–distribution, e.g. $\alpha' = 1\%$ leads to $\chi^2_{2,1-\alpha'} \approx 9.2$. Then

$$\alpha = 1 - \frac{H(\alpha')}{N} \tag{48}$$

with N being the number of all pixels involved. We now obtain a better compensation for the bias of $\beta^{(g)}$ namely

$$\hat{\beta} = c_2 \cdot \beta^{(g)} \tag{49}$$

$$\text{with} \quad c_2 = \frac{1}{1 + (1/\alpha - 1)\, ln(1 - \alpha)}\,. \tag{50}$$

(reducing to $1/(1 - ln2)$ for $\alpha = 0.5$, eq. (46)).
Remark: In principle this compensation process needed to be iterated until $\alpha' = \alpha$, as $H(\alpha')$ depends on the approximate values $\beta^{(h)}$. However usually only one iteration turned out to be necessary.
The final values for a and b are (cf. eg. (28))

$$\hat{a} = \hat{\beta}_1/t\,, \qquad \hat{b} = \hat{\beta}_2/t \tag{51}$$

with their variances

$$V(\hat{a}) = \frac{c_2^2}{t^2} \cdot V(\beta_1^{(g)})\,, \qquad V(\hat{b}) = \frac{c_2^2}{t^2} \cdot V(\beta_2^{(g)}) \tag{52}$$

For purposes of illustration we also determine the standard deviation σ_s and σ_l of the noise at the positions g_s and g_l (cf. eq. (11) and (31), (33)):

$$\hat{\sigma}_s = \sqrt{\hat{a} + \hat{b} g_s}\,, \qquad \hat{\sigma}_l = \sqrt{\hat{a} + \hat{b} g_l} \tag{53}$$

and their standard deviations $\sigma_{\hat{\sigma}_s}$ and $\sigma_{\hat{\sigma}_l}$.

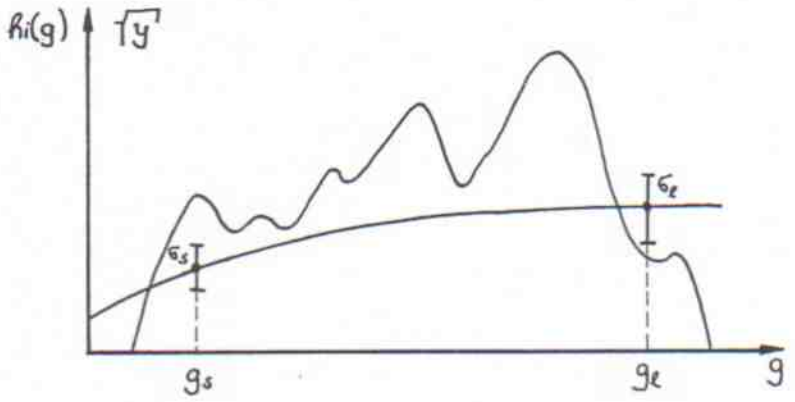

Figure 3: Histogram $hi(g)$ of gray–levels and standard deviation of noise

3.3 Experimental results

In order to verify the success of the preceding introduced noise estimating process we first tested it by artificially generated data. A random–number generator creates a set of 10000 equal distributed gray–levels g_i and a second random–number generator the corresponding y_i as χ^2_2–distributed values with signal dependent expectation values $E(y_i) = a + bg_i$, where a and b can be chosen. Then a certain percentage of y_i, e.g. 20% as in the first example (table (1)), is replaced by much higher values embodying edge pixels in the following way:

$$y_{i(edge)} = f^2(a + bg_i) \tag{54}$$

$$\text{with} \quad f \in \{f_{min} < f < f_{max}\}\,. \tag{55}$$

f as equal distributed factor fixes the contrast of an edge, whereby f_{min} can be chosen (we use: $f_{min} = 10$) and f_{max} depends on the used convolution kernels. Table (1) shows for varying noise parameters a and b the differences $da^{(0)} = |a - a^{(0)}|$, $db^{(0)} = |b - b^{(0)}|$ between given parameters and approximate values as well as the differences $da^{(1)} = |a - a^{(1)}|$, $db^{(1)} = |b - b^{(1)}|$ between given parameters and final estimates. Note that every experiment is repeated ten times with varying initial values for the random–number generators to receive mean values.

a	b	$da^{(0)}$ [%]	$db^{(0)}$ [%]	$da^{(1)}$ [%]	$db^{(1)}$ [%]
1	0.1	19.9 ± 5.8	40.7 ± 1.9	15.0 ± 3.4	5.4 ± 0.7
2	0.2	27.1 ± 4.8	44.1 ± 2.3	18.5 ± 5.5	8.1 ± 1.1
4	0.4	25.4 ± 5.1	36.5 ± 1.8	10.8 ± 2.5	5.1 ± 0.7

Table 1: Results from generated data

Tables (2) and (3) show some results of the noise estimating procedure on artificially generated images (figure (4): 9600 pixels, figure (5): 15800 pixels) which are disturbed with signal dependent noise, SNR is the signal–to–noise–ratio (σ_g/σ_n). Finally, the procedure is applied to real data, namely to the three color channels which are obtained by digitizing two aerial images with a red–, green– and blue–filter. (Size of the aerial images: 54000 and 62000 pixels). Table (4) illustrates the remarkable differences of noise in the three channels as well as its location dependency.

a	b	SNR	$da^{(0)}$ [%]	$db^{(0)}$ [%]	$da^{(1)}$ [%]	$db^{(1)}$ [%]
1	0.1	≈ 20	17.5 ± 5.1	22.0 ± 2.3	26.6 ± 4.5	5.2 ± 0.9
2	0.2	≈ 15	38.1 ± 7.5	13.1 ± 2.7	28.2 ± 5.4	3.3 ± 0.9
30	0.4	≈ 8	17.2 ± 4.0	13.2 ± 2.7	7.2 ± 2.8	5.6 ± 1.8

Table 2: Results from the generated image figure 4

a	b	SNR	$da^{(0)}$ [%]	$db^{(0)}$ [%]	$da^{(1)}$ [%]	$db^{(1)}$ [%]
1	0.1	≈ 16	28.8 ± 2.3	21.7 ± 7.3	25.1 ± 7.1	5.7 ± 1.6
2	0.2	≈ 11	24.0 ± 6.2	15.1 ± 1.4	15.4 ± 5.5	5.0 ± 0.9
30	0.3	≈ 7	14.3 ± 2.7	8.7 ± 2.5	8.5 ± 1.4	6.6 ± 1.3

Table 3: Results from the generated image figure 5

Figure 4:

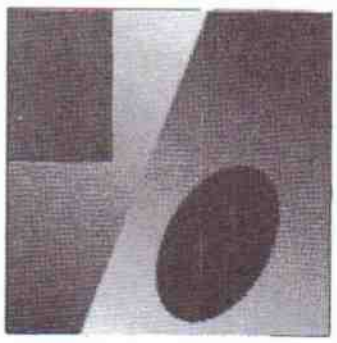

Figure 5:

	channel	SNR	$\hat{a}$	$\hat{b}$	$\hat{\sigma}_s$	$\hat{\sigma}_l$	$\sigma_{\hat{\sigma}_s}$	$\sigma_{\hat{\sigma}_l}$
image 1	red	≈ 8	4.53	0.25	3.40	6.93	0.07	0.32
	green	≈ 9	0.25	0.29	3.20	7.82	0.07	0.34
	blue	≈ 3	33.73	0.80	9.11	13.00	0.54	1.12
image 2	red	≈ 14	1.42	0.18	2.73	6.55	0.04	0.21
	green	≈ 21	2.34	0.09	2.42	4.85	0.03	0.12
	blue	≈ 5	62.98	0.59	9.59	13.70	0.49	1.12

Table 4: Estimated noise in 2 color images

4 Color edge extraction

Extracting edges from color images has to solve the problem how to merge the edge information in the different channels. This may be achieved by individually extracting edges from the individual channels and then joining this information using some logical operations, such as assuming an edge if one of the channels reveils an edge. Or the magnitude of the gradients of the different channels are added (cf. DREWNIOK 1988, CUMANI 1989), leading to an image which then may be handled as if resulting from a single channel image. The problem with both approaches is the ad hoc decision of the merging, as the possibly different significance of the individual channels is not taken into account.
Following the reasoning for the noise estimation, we assume the decision whether an edge is present or not as a hypothesis test: Only pixels being significantly non–homogeneous are candidats for edge pixels. This immedeately leads us to a mutual weighting of the different channels, which in principle may even take correlations between the channels into account. The essential conclusion from this assumption is: The channels are weighted according to the in general spatially varying noise (co–)variance, not according to the signal variance. We therefore want to use the homogeneity measures for the two homogeneity models A and B, discussed in section 2, adapt them to the task of edge or line extraction, apply them to RGB–color images and compare the results with respect to the influences of the location and channel variant noise variance.

4.1 Weigthing channels of multispectral images for edge extraction

We generalize the classical scalar measures used for monochrome images. In case of image model A, namely zero local slope nearly everywhere, the squared gradient

$$h^{2\,(A)} = g_r^2 + g_c^2 \tag{56}$$

is oftenly used. It may be written

$$h^{2\,(A)}(\mathbf{x}) = tr(\,\nabla g(\mathbf{x})\;\nabla g(\mathbf{x})^\top\,) = \frac{\partial g(\mathbf{x})}{\partial x_i}\cdot\frac{\partial g(\mathbf{x})}{\partial x_j}\cdot\delta_{ij}\,, \qquad i,j\in\{1,2\} \tag{57}$$

using $\mathbf{x} = (r, c) = (x_1, x_2)$ and Einsteins sum convention, summing over common indices. In order to compensate for spatially varying noise variance we need to normalize with the weight

$$w(\mathbf{x}) = 1/\sigma_n^2(\mathbf{x}) \tag{58}$$

and obtain the *normalized homogeneity measure for monochrome images:*

$$h^{2\,(A)}(\mathbf{x}) = \frac{\partial g(\mathbf{x})}{\partial x_i} \cdot \frac{\partial g(\mathbf{x})}{\partial x_j} \cdot \delta_{ij} \cdot w(\mathbf{x}) \,, \tag{59}$$

which is comparable to eq. (20) except for the used convolution kernels which are not specified here. In case $\mathbf{g}(\mathbf{x}) = (g_k(\mathbf{x}))$ is vector valued with $k = 1, \ldots, N_k$ channels we easily may generalize to the *normalized homogeneity measure for multispectral images*

$$h^{2\,(A)}(\mathbf{x}) = \frac{\partial g_k(\mathbf{x})}{\partial x_i} \cdot \frac{\partial g_l(\mathbf{x})}{\partial x_j} \cdot \delta_{ij} \cdot w_{kl}(\mathbf{x}) \,; \qquad i,j \in \{1,2\};\ \ k,l \in \{1,\ldots,N_k\} \tag{60}$$

with the spatially varying weight matrix (eq. (10))

$$\mathbf{W}(\mathbf{x}) = (w_{kl}(\mathbf{x})) = \left[\boldsymbol{\Sigma}_{nn}(\mathbf{x})\right]^{-1} = \left[\mathbf{A} + \mathbf{B}\big(\underline{f}(\mathbf{x})\big)\right]^{-1} . \tag{61}$$

In the special case of uncorrelated channels with $w_{kk} = w_k$ we obtain explicitely:

$$h^{2\,(A)}(\mathbf{x}) = \sum_{k=1}^{N_k} tr\big(\nabla g_k(\mathbf{x})\ \nabla g_k(\mathbf{x})^{\top}\big) / \big(a_k + b_k \underline{f}_k(\mathbf{x})\big) \,, \tag{62}$$

which reveils the simplicity of the generalization of eq. (57).
In a similar manner we may generalize a homogeneity measure under image model B, namely zero local curvature nearly everywhere. We use the generalization of the quadratic variation (GRIMSON, 1981)

$$h^{2\,(B)} = g_{rr}^2 + 2g_{rc}^2 + g_{cc}^2 \,. \tag{63}$$

It may be written as the trace of the square of the Hessian $\mathbf{H}(\mathbf{x}) = \big(\partial^2 g(\mathbf{x})/\partial x_i \partial x_j\big)$:

$$h^{2\,(B)}(\mathbf{x}) = tr\big(\mathbf{H}(\mathbf{x})\ \mathbf{H}^{\top}(\mathbf{x})\big) = tr\left[\left(\frac{\partial^2 g(\mathbf{x})}{\partial x_i \partial x_j}\right) \cdot \left(\frac{\partial^2 g(\mathbf{x})}{\partial x_j \partial x_n}\right)\right] = \frac{\partial^2 g(\mathbf{x})}{\partial x_i \partial x_j} \cdot \frac{\partial^2 g(\mathbf{x})}{\partial x_j \partial x_n} \cdot \delta_{in} \tag{64}$$

Again normalizing leads to

$$h^{2\,(B)}(\mathbf{x}) = \frac{\partial^2 g(\mathbf{x})}{\partial x_i \partial x_j} \cdot \frac{\partial^2 g(\mathbf{x})}{\partial x_j \partial x_n} \cdot \delta_{in} \cdot w(\mathbf{x}) \tag{65}$$

and in case of multispectral images results in

$$h^{2\,(B)}(\mathbf{x}) = \frac{\partial^2 g_k(\mathbf{x})}{\partial x_i \partial x_j} \cdot \frac{\partial^2 g_l(\mathbf{x})}{\partial x_j \partial x_n} \cdot \delta_{in} \cdot w_{kl}(\mathbf{x}) \,, \qquad i,j,n \in \{1,2\},\ k,l \in \{1,\ldots,N_k\} \tag{66}$$

with the same weight matrix eq. (61) as above. In case of uncorrelated channels this may be written as

$$h^{2\,(B)}(\mathbf{x}) = \sum_{k=1}^{N_k} \big(g_{rr,k}^2(\mathbf{x}) + 2g_{rc,k}^2(\mathbf{x}) + g_{cc,k}^2(\mathbf{x})\big) / \big(a_k + b_k \underline{f}_k(\mathbf{x})\big) \tag{67}$$

The homogeneity measure eq. (67) thus is a weighted quadratic variation, the weights depending on the spatially varying noise variance.
We only use image model A in the following.

4.2 Edge extraction procedure

The edge extraction procedure used for color images in the following experiment consists of the following steps:

1. determining the gradients and noise parameters of the individual channels
2. calculating the normalized homogeneity measure $h^{2\,(A)}(\mathbf{x})$ (cf. eq. (62)) at each pixel position
3. thresholding operation with the $\chi^2_{6,1-\alpha}$–fractil of the χ^2_6–distribution ($\alpha = 1\%$ leads to $\chi^2_{6,1-\alpha} \approx 16.81$) since the normalized homogeneity measure in case of three channels is χ^2_6–distributed, leading to homogeneous and boundary regions
4. non–maximum–suppression (according to CANNY (1986)) yielding local maxima as most probable edge pixels within the boundary regions
5. thinning algorithm (according to ROSENFELD and KAK (1981)) yielding a definite topology and a gridded binary image containing edge pixels.

4.3 Experimental results

In order to show that the above introduced color edge procedure is able to detect edges where a gray–level algorithm fails, we have digitized a picture of VASARELY containing color edges (from green to blue) with nearly the same intensities and a picture composed of colored paper areas. The figures (6)–(10) and (11)–(15) illustrate the different capabilities of both edge extraction procedures by showing the squared gradients as homogeneity measure of the individual channels and the intensity image (gray–level image) (cf. eq. (56)) as well as the normalized homogeneity measure of the color image (cf. eq. (62)). Observe the usefulness of the color information. Figure (8) shows very strong blue gradients because the picture of VASARELY contains edge information mainly in the blue spectral band. But the blue channel is the noisiest one so that it receives a small weight. That is the reason why the color gradients in this case are less strong than the blue gradients.

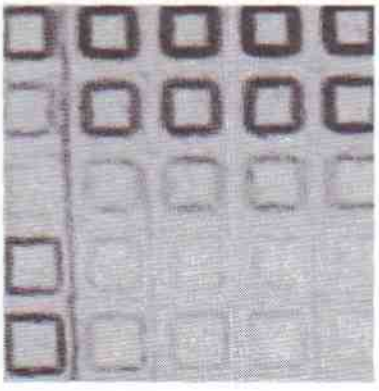

Figure 6: red gradients

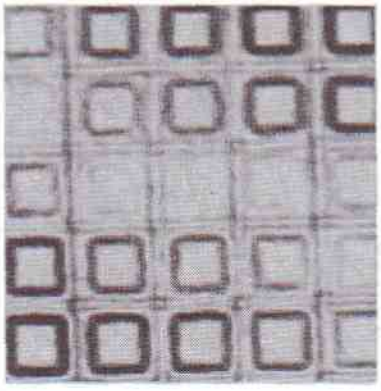

Figure 7: green gradients

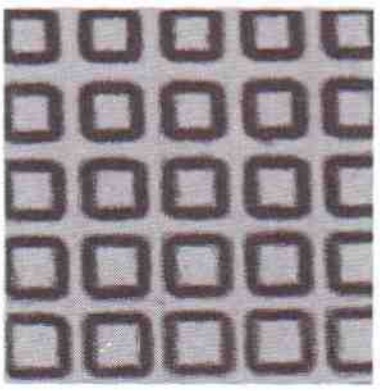

Figure 8: blue gradients

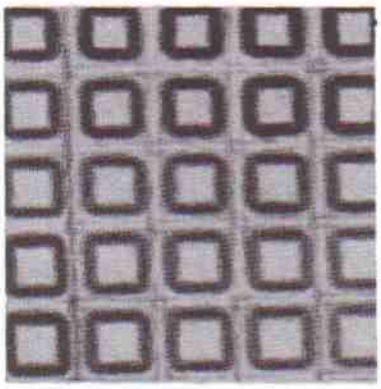

Figure 9: color gradients

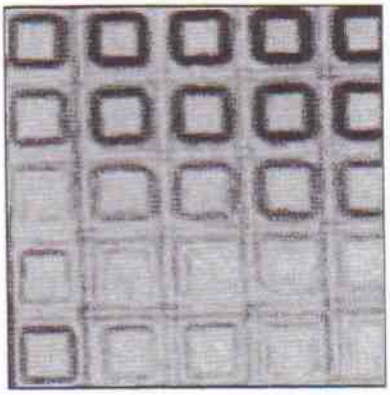

Figure 10: grey gradients

Figure 11:
red gradients

Figure 12:
green gradients

Figure 13:
blue gradients

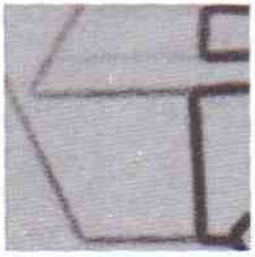

Figure 14:
color gradients

Figure 15:
grey gradients

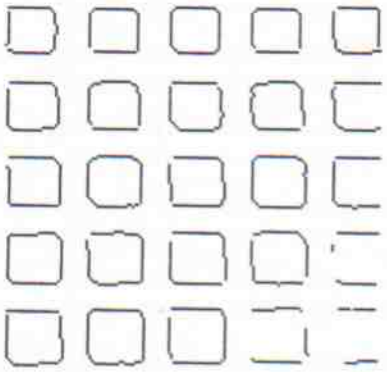

Figure 16:
fixed threshold a

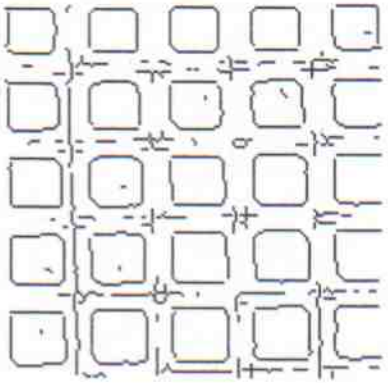

Figure 17:
fixed threshold b

Figure 18:
fixed threshold c

Figure 19:
variable threshold

Fig. (16)–(18) show a sequence of edge images derived from a color image using a *fixed* threshold in each image. Though by searching an acceptable threshold may be found, the result of the noise estimation in the three channels immediately leads to the edge image in fig. (19), demonstrating no interactivity to be necessary, also in this complicated case.

5 Conclusions

The paper presented a model for the noise variance based on the Poisson statistic of the photon flux and additional signal independent noise components. A procedure has been developed to robustly estimate the variance components in the presence of edges. The accuracy of the estimated standard deviations of the noise variances are in the range of 5–20%, which is fully sufficient for automatically adapting tresholds to the image dependent noise characteristics. The estimation process also yields an internal estimate for the achieved precision.

The applicability of the approach has been demonstrated with simulated and real mono-

monochrome and color images. No thresholds have to be provided once a significance level has been fixed, allowing to handle single multispectral images with unknown noise variance components. The pocedure has to be supplemented by a test on the suitability of the assumed linear variance model, in case the sensor has to be expected to have nonlinear (e.g. logarithmic) transfer characteristic.
Further research is necessary to model the joint noise properties of digital images resulting from scanned photographic film.

6 Literature

CANNY J. (1986) : A Computional Approach to Edge Detection, IEEE T–PAMI 8, No. 6, pp.678-698

CHEN P.C., PAVLIDIS T. (1981) : Image Segmentation as an Estimation Problem in Image Modeling, in: Image Modeling, pp. 9-28

CUMANI A. (1989) : Edge Detection in Multispectral Images, CVGIP 53, 1991, pp. 40-51

DE SOUZA P. (1983) : Edge Detection Using Sliding Statistical Tests, CVGIP 23, 1983, pp. 1-14

DREWNIOK C. (1988) : Untersuchungen zur Detektion von Kanten in digitalen Farbbildern, Bericht FBI-HH-B-138/88, Universität Hamburg, Fachbereich Informatik, 1988

FÖRSTNER W.(1991) : Statistische Verfahren für die automatische Bildanalyse und ihre Bewertung bei der Objekterkennung und –vermessung, Deutsche Geodätische Kommission, Reihe C, Heft Nr. 370, München, 1991

GRIMSON W.E.L. (1981) : From Image to Surfaces, MIT press 1981, chapter 6

HARALICK R.M. (1981) : Edge and Region Analysis for Digital Image Data, in: Image Modeling, pp. 171-184

HSU Y.Z., NAGEL H.-H., REKERS G. (1984) : New Likelihood Test Methods for Change Detection in Image Sequences, CVGIP 26, 1984, pp. 73-106

NEVATIA R. (1977) : A color edge detector and its use in scene segmentation, IEEE Trans. Systems Man Cybernet SMC-7, 1977, pp. 820-826

NEYMAN J., PEARSON E.S. (1933) : On the Problem of the Most Efficient Tests of Statistical Hypothesis, Phil. Trans. Royal Soc. London, Series A, 231, 289 (1933)

ROSENFELD A. (1981, ED.) : Image Modeling, Academic Press, INC 1981

ROSENFELD A., KAK A. (1981) : Digital Picture Processing, Academic Press, INC, volume 2, pp. 232-240

SHIOZAKI A. (1986) : Edge extraction using entropy operator, Computer Vision, Graphics and Image Processing 36, 1986, pp. 1-9

SOLINSKY J.C. (1985) : The Use of Color in Machine Edge Detection, Proc. VISION-85, Detroit, MI, 1985, pp. 25-28

SUK M. (1984) : An Edge Extraction Technique for Noisy Images, CVGIP 25, 1984, pp. 24-45

TORRE V., POGGIO T. (1986) : On edge detection, IEEE Transactions on Pattern Analysis and Machine Intelligence PAMI-8, 1986, pp. 147-163

YAKIMOVSKY Y. (1976) : Boundary and Object Detection in Real World Images, Journal of the ACM 23, 1976, pp. 599-618